PNAS RESEARCH ARTICLE | DEVELOPMENTAL BIOLOGY OPEN ACCESS

Hatching is modulated by microRNA-378a-3p derived from extracellular vesicles secreted by blastocysts

Krishna Chaitanya Pavani[a,b,1,2], Tim Meese[c,1], Osvaldo Bogado Pascottini[a,d], XueFeng Guan[e], Xiaoyuan Lin[e], Luc Peelman[e], Joachim Hamacher[f], Filip Van Nieuwerburgh[c], Dieter Deforce[c], Annekatrien Boel[g], Björn Heindryckx[g], Kelly Tilleman[b], Ann Van Soom[a], Bart M. Gadella[h], An Hendrix[i,j], and Katrien Smits[a,2]

Edited by Thomas Spencer, University of Missouri, Columbia, MO; received December 21, 2021; accepted February 4, 2022

Extracellular vesicles (EVs) and their cargo microRNAs (miRNAs) are important regulators of embryo development to the blastocyst stage and beyond. Before implantation can take place, hatching of blastocysts from their zona pellucida is required. However, underlying mechanisms by which blastocyst formation and hatching are initiated remain largely unknown. Here, we provide evidence that embryonic EVs containing bta-miR-378a-3p play a crucial role in blastocyst hatching, using a bovine model. A customized procedure was used to isolate EV-miRNAs from culture droplets conditioned by individual bovine embryos that either developed to the blastocyst stage or did not (nonblastocyst). RNA sequencing identified 69 differentially expressed miRNAs between EVs derived from blastocyst conditioned medium (CM) and nonblastocyst CM. Among the miRNAs up-regulated in blastocyst CM, we selected bta-miR-378a-3p for further validation by functionality testing on developing in vitro embryos by means of mimics and inhibitors. Supplementing the embryo culture medium with miR-378a-3p mimic significantly improved blastocyst quality, with higher cell numbers and reduced apoptosis, and improved hatching, while the opposite was found after supplementation with miR-378a-3p inhibitor ($P < 0.01$). Transcriptomic analysis of embryos treated with miR-378 mimic/inhibitor showed differential expression ($P < 0.01$) of genes associated with embryo development and implantation, including *RAP1GAP*, *ARFGEF2*, *SLC7A6*, *CENPA*, *SP1*, *LDLR*, *PYCR1*, *MYD88*, *TPP1*, and *NCOA3*. In conclusion, miR-378a-3p is up-regulated in EVs secreted by embryos that develop to the blastocyst stage, and this EV-derived miR-378a-3p increases blastocyst quality and regulates embryo hatching, which is essential for embryo implantation.

extracellular vesicles | miRNAs | blastocyst | hatching

Significance

Hatching from the zona pellucida is a prerequisite for embryo implantation and is less likely to occur in vitro for reasons unknown. Extracellular vesicles (EVs) are secreted by the embryo into the culture medium. Yet the role that embryonic EVs and their cargo microRNAs (miRNAs) play in blastocyst hatching has not been elucidated, partially due to the difficulties of isolating them from low amounts of culture medium. Here, we optimized EV-miRNA isolation from medium conditioned by individually cultured bovine embryos and subsequently showed that miR-378a-3p, which was up-regulated in EVs secreted by blastocysts, plays a crucial role in promoting blastocyst hatching. This demonstrates the regulatory effect of miR-378-3p on hatching, which is an established embryo quality parameter linked with implantation.

Mammalian fertilization represents the beginning of a new life. In many species, embryo development can now partially take place in vitro, following a strict timeline of developmental milestones (1). After in vitro fertilization and the first cleavage divisions, the embryonic cells will compact at the morula stage, and, next, they will segregate into the inner cell mass (ICM) cells, representing the embryo proper, with the cavity inside and the trophectoderm (TE, founder of the placenta) on the outside of the so-called blastocyst. Until the blastocyst stage, the embryo is protected by the zona pellucida, a glycoproteic layer. Then, the blastocyst will repeatedly expand and collapse to escape from the zona pelllucida, thereby initiating a process called hatching (2). Successful hatching is an indication for embryo quality, and a prerequisite before implantation can take place (3). However, while in vivo–derived embryos exhibit very high hatching rates (4), blastocysts produced in vitro often fail to hatch, and implantation failure accounts for 75% of all pregnancy losses after human IVF (5) and more than 50% after bovine IVF (4). Assisted hatching after IVF can improve pregnancy rates by 25%, illustrating the importance of embryo hatching (3, 6). Yet, underlying mechanisms and signaling molecules affecting blastocyst formation and hatching remain largely unknown.

Among a plethora of signaling factors, interesting candidates that have been shown to modulate embryo development, as well as to be released by embryos, are extracellular vesicles (EVs) (7). EVs are 50- to 300-nm-sized membrane vesicles that carry regulatory molecules such as microRNAs (miRNAs), messenger RNAs (mRNAs), lipids, metabolites, and proteins (8–10). The first study on embryonic EVs showed that in vitro–produced porcine parthenogenetic embryos release EVs (11). Later, it was demonstrated that EVs extracted from medium conditioned by bovine oviduct epithelial cells enhanced bovine blastocyst quality (12). Our own recent research indicated that bovine embryos cultured in vitro in a group release functionally active EVs that positively influence the development of bovine embryos cultured individually (7). The

Author contributions: K.C.P., D.D., K.T., A.V.S., B.M.G., A.H., and K.S. designed research; K.C.P., T.M., X.G., X.L., J.H., and A.B. performed research; K.C.P., T.M., A.V.S., and A.H. contributed new reagents/analytic tools; K.C.P., T.M., O.B.P., L.P., F.V.N., B.H., A.V.S., B.M.G., A.H., and K.S. analyzed data; and K.C.P., K.T., A.V.S., B.M.G., and K.S. wrote the paper.

The authors declare no competing interest.

This article is a PNAS Direct Submission.

[1]K.C.P. and T.M. contributed equally to this work.

[2]To whom correspondence may be addressed. Email: Krishnachaitanya.Pavani@UGent.be or Katrien.Smits@UGent.be.

This article contains supporting information online at http://www.pnas.org/lookup/suppl/doi:10.1073/pnas.2122708119/-/DCSupplemental.

Published March 17, 2022.

EVs released by individually cultured preimplantation bovine embryos can even alter the gene expression of oviduct epithelial cells (13) and endometrial cells (14). These data underline the crucial role of embryo derived EVs in embryo–embryo and embryo–maternal communication. Moreover, EVs can contain important signaling molecules, like miRNAs. As the membrane of EVs can effectively protect enclosed cargo contents (miRNA, mRNAs) from RNase present in the medium, miRNAs derived from EVs are more stable and reliable than free-floating miRNAs (15, 16). Until now, only a few studies have been conducted on miRNAs isolated from conditioned media (CM) generated by group cultured blastocysts or degenerated embryos, and they suggested a link with embryo quality and development (17, 18). Yet, the function of miRNAs derived from EVs secreted by individually cultured embryos has not yet been studied, partially due to the difficulty of isolating EVs from such low concentrate–low volume samples.

Here, we analyzed the difference in the repertoire of miRNAs in EVs isolated from medium conditioned by bovine blastocysts vs. nonblastocysts, using next-generation sequencing, involving a total of 660 individually cultured embryos. We identified miR-378a-3p as being specifically present in EVs secreted by blastocysts and absent in nonblastocysts. Moreover, by means of functional assays using inhibitors and mimics for miR-378a-3p, we showed that EV-derived miR-378a-3p significantly affects embryo quality and hatching and alters the expression of genes involved in embryo development, hatching, and implantation.

Results

EV Morphology and Concentration Can Differentiate Blastocysts and nonblastocysts. To characterize EVs, we collected and pooled 120 individual droplets of media conditioned by embryos that had either reached the blastocyst stage or not (nonblastocysts) after being cultured from the zygote stage in synthetic oviductal fluid (SOF)+ Insulin, transferrin, selenium (ITS)+ bovine serum albumin (BSA) medium until 8 d post insemination (dpi). The fractions enriched for EVs (6–15) were extracted using size exclusion chromatography (SEC) (qEV single column^{TM}), and the morphology and size distribution of EVs were evaluated by transmission electron microscopy (TEM) and nanoparticle tracking analysis (NTA). Western blot confirmed the presence of EV-specific markers (CD63, CD9, and TSG101) in the EV samples derived from blastocyst and nonblastocyst CM (Fig. 1*A* and *SI Appendix*, Figs. S1 and S2), while AGO-2 and ApoA-I, negative markers of EVs, were absent (Fig. 1*A*).

When comparing blastocyst EVs with nonblastocyst EVs, Western blot data showed an enrichment of CD9 and TSG101 in blastocyst EVs (Fig. 1*A*) even though an equal sample volume was loaded during the Western blot process. This indicates a higher concentration of EVs in the blastocyst-derived samples compared to the nonblastocysts (19). Similarly, by NTA, a higher particle concentration was observed in blastocyst EVs ($94.5 \pm 1.7 \times 10^8$ particles per mL) compared to nonblastocyst EVs ($76.5 \pm 8.2 \times 10^8$ particles per mL) ($P < 0.05$) (Fig. 1*B*). Blastocyst EVs were also characterized by larger particle sizes with a mean diameter of 147.4 ± 16.4 nm, whereas nonblastocyst EVs displayed smaller particle sizes with a mean diameter of 118.3 ± 6.1 nm ($P < 0.05$). TEM confirmed the presence of larger-sized vesicles in blastocyst EVs (≥200 nm) (Fig. 1*C*).

Customized EV Isolation Procedure Proves to Be Effective for RNA Isolation. In order to be able to isolate total RNA from EVs collected from CM, we used smaller aliquot volumes of CM for isolating EVs by SEC (qEV single column) followed by a series of concentration steps prior to RNA extraction (7, 20). This optimized method resulted in a desirable RNA concentration (101 pg/μL to 356 pg/μL), absence of ribosomal RNA, and enrichment of small (<200 nt) RNA species for all the samples (*SI Appendix*, Fig. S3). To further characterize the RNA content of these EVs, we performed RNA sequencing (RNA-seq) on these total RNA samples. After sequencing, 590 miRNAs were detected in both blastocyst and nonblastocyst EVs.

miRNAs Derived from Blastocyst EVs Regulate Embryo Development and Quality. We identified 69 differentially expressed (DE) miRNAs between blastocyst and nonblastocyst EVs, with 21 known miRNAs (19 up-regulated and 2 down-regulated; *SI Appendix*, Table S1) and 48 potential novel miRNAs (18 up-regulated and 30 down-regulated; *SI Appendix*, Table S2). For 26 DE novel miRNAs, homologs in other species were identified, and the remaining 22 novel miRNAs have yet to be annotated (*SI Appendix*, Table S2). Hierarchical clustering analysis confirmed categorization of DE miRNAs into nonblastocyst EVs and blastocyst EVs (Fig. 2*A*). By performing sequence annotation pipeline analysis on known and novel DE miRNAs, we identified two DE miRNAs (bta-miR-151-5p and bta-miR-151-3p) that are up-regulated in blastocyst EVs and are clustered in the same region of chromosome BTA14 (Chr 14; *SI Appendix*, Table S3). These two miRNAs share a primary transcript, which is also reflected in the coordinates (same chromosome and start and stop positions very close to each other). Similarly, two novel DE miRNAs (bta-novel-miR-231, bta-novel-miR-462) up-regulated in blastocyst EVs are clustered in the same region of chromosome BTA 21 (Chr 21; *SI Appendix*, Table S4). We also identified five novel DE miRNAs (bta-novel-miR-19, bta-novel-miR-33, bta-novel-miR-326, bta-novel-miR-342, and bta-novel-miR-360) with matched bovine seed regions, that are up-regulated in nonblastocyst EVs and clustered in the same region of the chromosome (Chr 7; *SI Appendix*, Table S4). By using the miRBase database, we matched DE miRNAs with miRNA gene families, and we could identify that two known miRNAs (bta-miR-25 and bta-miR-92b) were connected to the same family (miR-25) and that three miRNAs (bta-miR-151-3p, bta-miR-151-5p, and bta-miR-28) also belong to the same family (miR-28) (*SI Appendix*, Table S1). For the novel miRNAs, we found bta-novel-miR-163 and bta-novel-miR-164 belonging to the miR-1421 family, while both bta-novel-miR-81 and bta-novel-miR-82 belong to the miR-130 family (*SI Appendix*, Table S2). Only one known miRNA (bta-miR-11986b) was missing gene families, as no matched seed region could be found in miRbase (*SI Appendix*, Table S1).

To assess the DE miRNA–target interactions, we used miRanda to predict targets based on the genome of Bos Taurus. The results revealed that 4,346 genes were targeted by DE known and novel miRNAs of blastocyst and nonblastocyst EVs. For these target genes, simplifyEnrichment analysis revealed Gene Ontology (GO) gene sets enriched in cell development, signaling pathway response, cell differentiation, cellular proliferation, cell survival, endosomes, plasma membrane receptor, vesicles, ion binding, kinase activity, and channel regulator activity (Fig. 2 *B*–*D*). Additional analysis of the top 10 enriched Kyoto Encyclopedia of Genes and Genomes (KEGG) and GO pathways displayed a similar output (as detailed in *SI Appendix*, Fig. S4). These data showed that miRNAs in

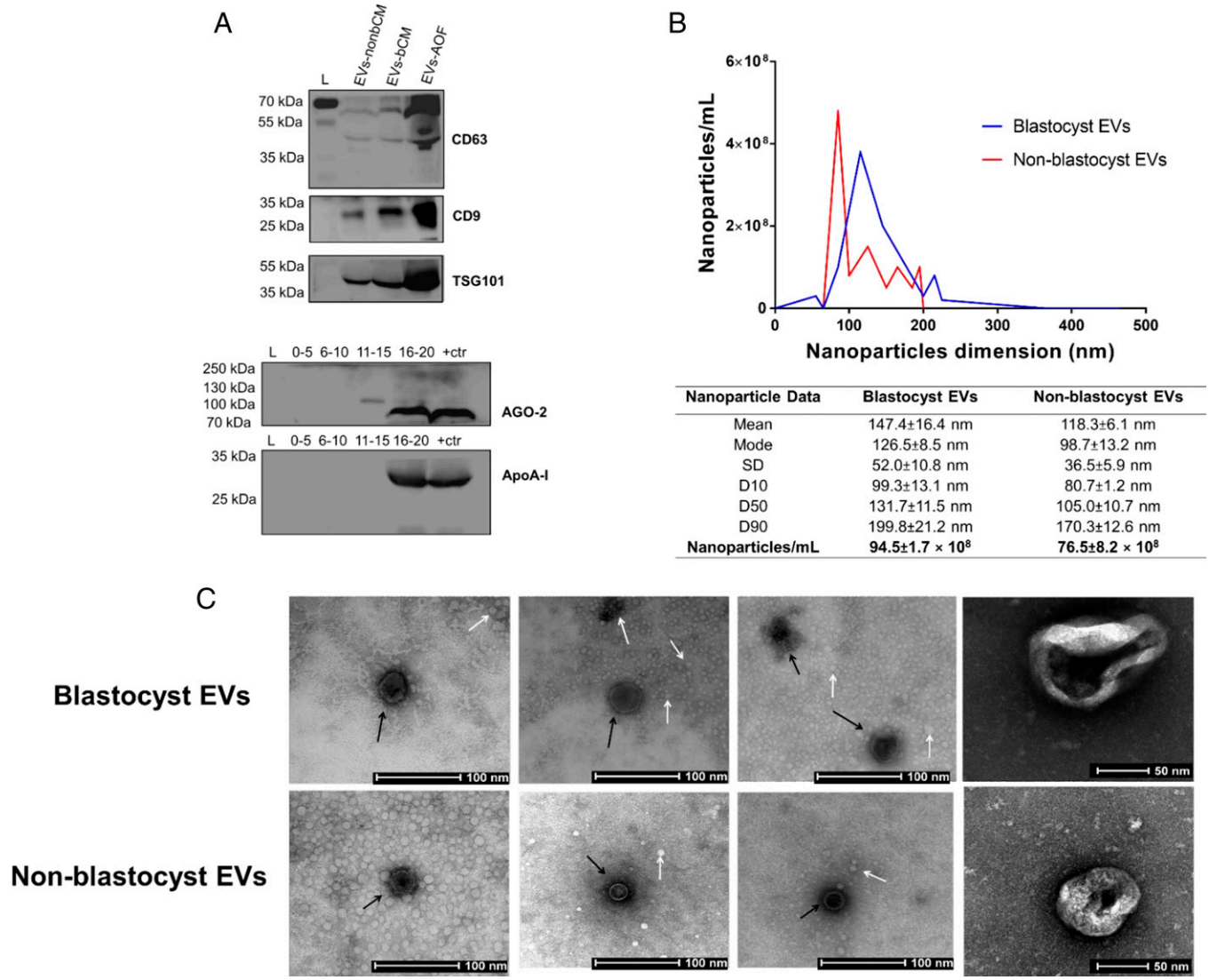

Nanoparticle Data	Blastocyst EVs	Non-blastocyst EVs
Mean	147.4±16.4 nm	118.3±6.1 nm
Mode	126.5±8.5 nm	98.7±13.2 nm
SD	52.0±10.8 nm	36.5±5.9 nm
D10	99.3±13.1 nm	80.7±1.2 nm
D50	131.7±11.5 nm	105.0±10.7 nm
D90	199.8±21.2 nm	170.3±12.6 nm
Nanoparticles/mL	**94.5±1.7 × 10⁸**	**76.5±8.2 × 10⁸**

Fig. 1. Identification and characterization of EVs isolated from the blastocyst and nonblastocyst CM. (*A*) Western blotting analysis of the EVs shows that blastocyst (b) and nonblastocyst (nonb) CM and ampullary oviduct fluid (AOF) expressed traditional EV-associated markers CD63 (42 kDa), CD9 (25 kDa), and TSG101 (49 kDa). Non-EV markers AGO 2 (87 kDa) and ApoA-I (28 kDa) were absent in EV-enriched fractions (6 to 15) derived from blastocyst CM by SEC (qEV single step), while they were expressed in SEC fractions 16 to 20 and positive control (pure embryo CM). (*B*) Size distribution of blastocyst and nonblastocyst EVs by NTA indicates a larger size for blastocyst EVs. The mode, mean value, and SD of size and concentration are provided for each EV isolation. The value D50 represents the median size. Similarly, 90% of the distribution lies below the D90 value, and 10% of the population lies below the D10 value. (*C*) Transmission electron micrograph of the blastocyst and nonblastocyst EVs demonstrates vesicles with sizes ranging from 50 nm to 250 nm in diameter. EVs (black arrows) and amorphous material (white arrows) are indicated. (Scale bar: 100 nm or 50 nm.)

blastocyst EVs are highly relevant in embryo development and quality.

miRNA-378a-3p Is Located inside EVs Secreted by Blastocysts. Among all DE miRNAs, miRNA-378a-3p (hereinafter referred to as miR-378) was selected for further validation based on its association with blastocyst-derived EVs and on evidence from literature indicating a role in cell growth, cellular proliferation, and embryo implantation (Table 1). Firstly, the EV origin of miR-378 was confirmed. The RNA concentration was slightly decreased for EVs treated with Proteinase K and RNase A, when compared to untreated EVs (control) (about 10%; *SI Appendix*, Fig. S5 *A* and *B*). Addition of detergent (Nonidet P-40) along with Proteinase K and RNase A resulted in a greater decline in the RNA concentration (about 58%; *SI Appendix*, Fig. S5*B*). The RNA concentration was also determined in samples where RNA was extracted directly from the blastocyst CM. For both treatment groups (Proteinase K and RNase A, Proteinase K and RNase A, along with Nonidet P-40), the RNA concentration was significantly decreased compared with the control (about 48% and 62%, respectively; *SI Appendix*, Fig. S5*B*).

For qRT-PCR normalization, two reference miRNAs (bta-miR-93 and bta-miR-127b) were selected (21), but only bta-miR-93 was stably expressed at different concentrations and retained for further analysis. Expression of miR-378 was determined by qRT-PCR for the different treatment groups. When EVs were treated with Proteinase K and RNase A, but not with Nonidet P-40, the PCR signal for the miR-378 remained similar to the control. This indicates that miR-378 captured by the qEV column was located inside the vesicles and therefore protected, by the lipid bilayer, from Proteinase K and RNase A digestion (*SI Appendix*, Fig. S5*C*). Treating EVs with Proteinase K and RNase along with Nonidet P-40 led to the digestion

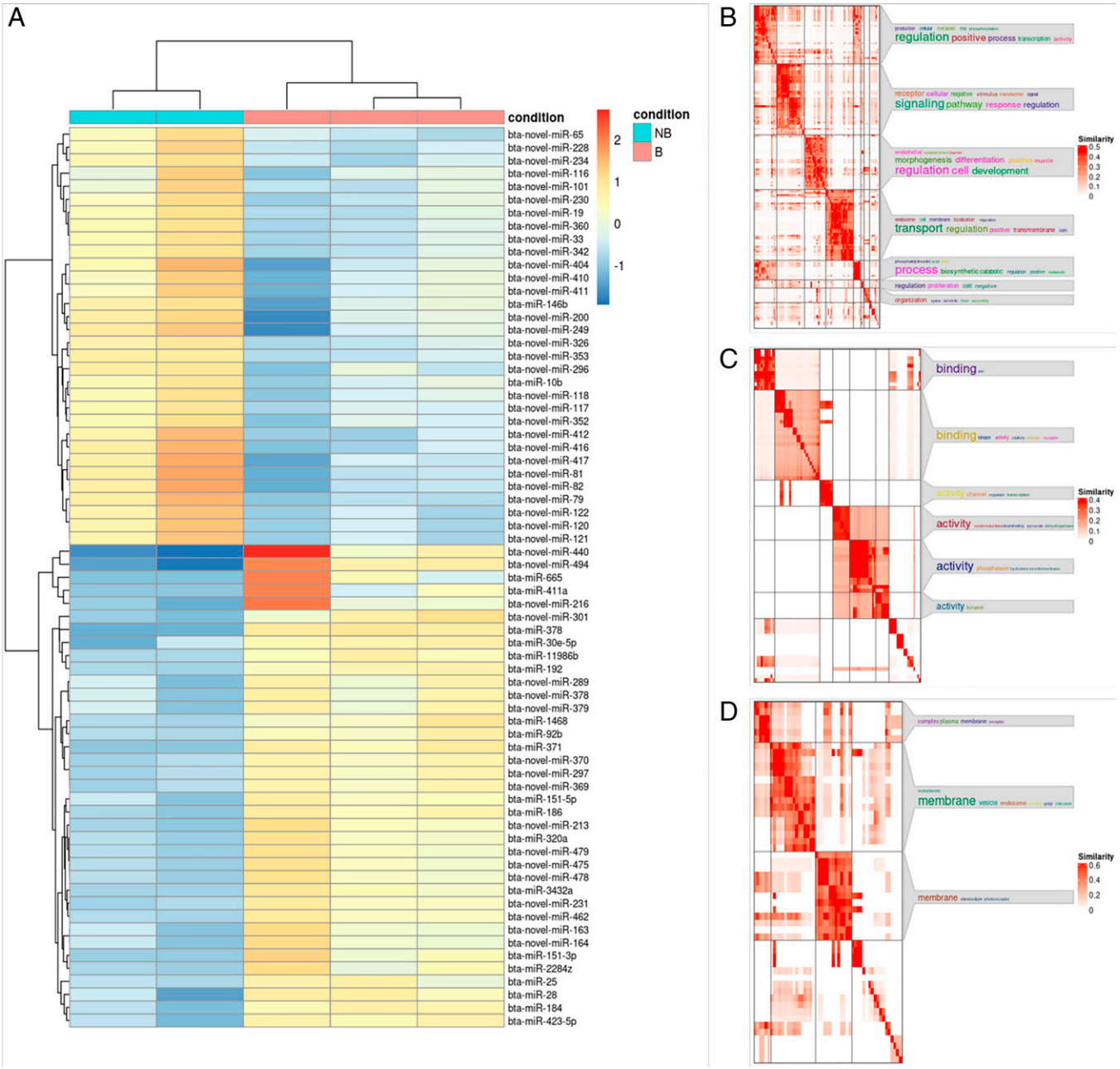

Fig. 2. EV-derived miRNA profiles of medium conditioned by blastocysts (B) and nonblastocysts (NB). (*A*) Heatmap generated by clustering of the DE miRNAs in blastocyst and nonblastocyst EVs. Red, up-regulation; blue, down-regulation as compared to the mean expression over all samples. (*B–D*) GO enrichment of DE miRNAs. Semantic similarities scores were calculated between all significant GO terms with their respective category (biological process [BP], cellular component [CC], and molecular function [MF]) with Schlicker's Relevance method. The resulting GO terms were clustered by binary cut enriched and categorized by (*B*) BP, (*C*) MF, and (*D*) CC.

of RNAs (*SI Appendix*, Fig. S5*B*), confirming that their initial resistance to digestion was due to impounding within vesicles, which proved miR-378 to be inside of the blastocyst EVs.

miRCURY Locked Nucleic Acids (LNA) miRNA Mimics Are Taken up by Embryos. Before examining the functionality of candidate miR-378, we first tested whether the commercially available triple-RNA-strand mimics can pass through the zona pellucida of bovine embryos. In order to confirm internalization of these mimics, we supplemented fluorescently labeled miRNA mimics or phosphate-buffered saline (PBS) to in vitro culture medium of presumed zygotes at 1 dpi. After 24 h, fluorescence microscopy showed that mimics were able to cross the zona pellucida, whereas the PBS control showed no signal (Fig. 3*A*). Notably, these triple-RNA-strand labeled mimics were stable until 8 dpi (Fig. 3*B*), confirming uptake of these mimics by embryos without performing microinjection.

miR-378 Mimics and Inhibitors Modulate Hatching and Embryo Quality. To further determine the effect of miR-378 on embryo development, we supplemented miR-378 mimics or inhibitors to the culture medium containing presumed zygotes at 1 dpi and cultured them until day 8, thus allowing miR-378 mimics or inhibitors to influence further embryo development. While cleavage and blastocyst rates were not affected, supplementation of miR-378 mimics resulted in an increased hatching rate

Table 1. Literature indicating involvement in embryo development of the selected miRNA for qRT-PCR verification

miR_ID	hsa-miR-378a-3p
References (PMID)[a]	18077375,19844573,21242960;2124296021471220, 21846797,23447532, 23333942, 23625957, 23625957, 23625957, 27855367, 2515062227001906, 26313654, 2625581626749280, 27832641
Target gene	*SUFU*, *NPNT*, *MYC*, *TOB2,MSC*, *CYP19A1*, *GRB2*, *CDK6*, *IGF1R*, *KSR1*, *MAPK1*, *TGFB2*, *PGR*, *GLI3*, *NKX3-1GOLT1A*, *RUNX1*, *WNT10A*
Target genes functionality (Entrez ID)	Cell growth, cellular proliferation, cell adhesion, cell cycle progression, cell survival, embryo implantation, protein binding

[a]PMID: PubMed unique identifier

(22.6 ± 3.6) in comparison to the control (10.7 ± 2.6) and negative control (NC) mimic (12.5 ± 2.4) groups ($P = 0.004$) (Table 2). In line with these findings, supplementation with the miR-378 inhibitor resulted in a much lower hatching rate (1.0 ± 1.1) compared to the control group (10.8 ± 2.0) ($P = 0.002$). Furthermore, differential apoptotic staining indicated a beneficial effect of miR-378 on embryo quality (Table 3). Notably, blastocysts cultured in the presence of miR-378 mimics had a higher number of ICM cells (60.1 ± 3.1) than all other groups ($P = 0.0003$). Also, the total cell number (TCN) was greater ($P < 0.05$) for blastocysts cultured with miR-378 mimics (149 ± 9.5) than the control (123 ± 9.5). Similarly, supplementation with the miR-378 inhibitor resulted in a lower TCN (88.3 ± 8.9) and ICM (38.8 ± 3.6) than the nonsupplemented control

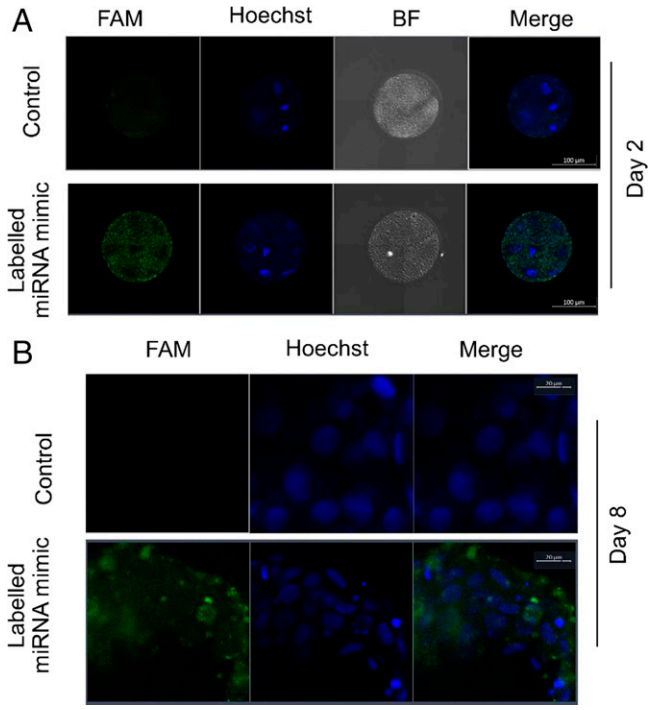

Fig. 3. Bright-field and fluorescence images demonstrating the passage of miRNA mimics through the zona pellucida and the subsequent miRNA mimics uptake by the cells of the blastocyst. Commercial triple-RNA-strand mimics were prelabeled with 5′ FAM (5-carboxyfluorescein) and supplemented to the in vitro culture medium at 1 dpi along with PBS (control) and cultured until 8 pdi. (*A*) At 2 dpi, zona-intact bovine embryos along with labeled mimics (5′ FAM, green) or PBS were washed, fixed, and stained with Hoechst (blue) to visualize the nuclei. The merged image demonstrates uptake of green fluorescent–labeled mimics by zona-intact embryos at 2 dpi. A control with PBS coincubated with bovine embryos did not show any green fluorescence. (*B*) Similarly, at 8 dpi, blastocysts were collected and washed, fixed, and stained with Hoechst (blue) to visualize the nuclei. The merged images also demonstrate the uptake of labeled mimics by blastocysts even at 8 dpi.

(120 ± 7.9 and 52.3 ± 3.2, respectively) ($P = 0.008$), but this was not significant when compared to the supplementation with NC inhibitor. Interestingly, the apoptotic cell (AC) number and AC ratio (AC/TCN) were greater in the miR-378 inhibitor group (10.2 ± 1.2 and 12.6 ± 1.0, respectively) compared to the control (6.0 ± 1.0 and 4.9 ± 0.9, respectively) ($P < 0.05$). These results indicate that miR-378 contributes to embryo growth, embryo quality, and hatching. Hereinafter, embryo treatment groups will be referred to as control, NC mimic, NC inhibitor, miR-378 mimic, and miR-378 inhibitor.

Higher miR-378 Expression Is Associated with Improved Embryo Quality. The miR-378 expression levels were compared by qRT-PCR in blastocysts vs. nonblastocysts vs. in the EVs released by the blastocysts and nonblastocysts, using both an individual and a group culture system (*SI Appendix*, Fig. S6). This confirmed the higher expression of miR-378 in blastocyst-derived EVs, compared to EVs derived from arrested embryos. Interestingly, the miR378 content in the blastocysts was also higher, compared to nonblastocysts ($P < 0.001$). Yet, miR-378 levels in the embryos and in the EVs released by these embryos were not statistically different. Strikingly, miR-378 levels were significantly higher in embryos cultured in a group compared to individual culture ($P < 0.0002$), again demonstrating the link between miR-378 and hatching, as hatching rates were significantly higher in group culture when compared to individual culture (7).

miR-378 Mimics and Inhibitors Modulate the Transcriptome Profile of Blastocysts. To gain more in-depth molecular insights, we performed transcriptome profiling of blastocysts cultured in the presence of miR-378 mimics or inhibitors. The effect of miR-378 mimics was determined for three comparisons (control vs. NC mimic; control vs. miR-378 mimic, and NC mimic vs. miR-378 mimic), resulting in a total of 238 DE genes. Comparison of both control groups (control vs. NC mimic) showed 80 DE genes, indicating some phenotypic influence on the embryos of the NC mimic. Therefore, the 20 common DE genes in control vs. NC mimic were excluded from further comparison between miR-378 mimics and both control groups (Fig. 4*A*). As such, a total of 158 DE genes were identified in the miR-378 mimic supplemented group compared to both controls (Dataset S1). Supplementation of miR-378 mimic resulted in 58 DE genes (29 up and 29 down) compared to the nonsupplemented control, and 89 DE genes (48 up and 41 down) compared to the NC mimic, while 11 common DE genes were found for the miR-378 mimic group compared to both control groups (*SI Appendix*, Table S5).

Further transcriptional analysis of blastocysts from the miRNA-378 inhibitor treatment groups (control vs. NC

Table 2. Blastocyst development and hatching rates of bovine embryos treated with miRNA mimics/inhibitors

Treatment	No. of presumed zygotes	Cleavage rate (%)	Blastocyst rate 7 dpi (%)	Blastocyst rate 8 dpi (%)	Hatched/hatching per presumed zygotes (%)	Hatched/hatching per 8 dpi blastocysts (%)
Control	161	88.6 ± 2.9[a]	42.2 ± 4.8[a]	49.7 ± 3.9[a]	10.7 ± 2.6[a]	22.1 ± 4.9[ab]
NC mimic	225	90.1 ± 2.5[a]	37.4 ± 4.1[a]	46.2 ± 3.3[a]	12.5 ± 2.4[a]	27.3 ± 4.8[a]
miRNA-378 mimic	171	92.8 ± 2.2[a]	41.3 ± 4.7[a]	49.1 ± 3.8[a]	22.6 ± 3.6[b]	46.5 ± 5.9[b]
Control	239	88.3 ± 2.0[a]	39.2 ± 3.7[a]	45.5 ± 4.5[a]	10.8 ± 2.0[a]	22.6 ± 3.9[a]
NC inhibitor	165	89.7 ± 2.3[a]	29.7 ± 3.6[a]	32.2 ± 4.8[a]	6.0 ± 1.8[ab]	17.2 ± 4.9[ab]
miRNA-378 inhibitor	194	90.2 ± 2.1[a]	30.4 ± 3.5[a]	37.7 ± 4.9[a]	1.0 ± 1.1[b]	6.1 ± 2.6[b]

Cleavage, 7 and 8 dpi blastocyst rates, and hatched/hatching rates expressed as a percentage of presumed zygotes. For the miRNA mimic experiment, culture media were not supplemented (Control), or were supplemented with control mimics (NC mimics) or with miRNA-378 mimics. For the miRNA inhibitor experiment, culture media were not supplemented (Control), or were supplemented with control inhibitors (NC inhibitor) or with miRNA-378 inhibitor. Different superscripts per column (a and b) represent statistical differences ($P < 0.05$) among treatments. Results are expressed as least-square mean ± SE.

inhibitor; control vs. miR-378 inhibitor, and NC mimic vs. miR-378 inhibitor) resulted in the identification of a total of 297 DE genes. As observed above, 102 DE genes were found in the comparison of control vs. NC inhibitor. Therefore, the 29 DE genes from control vs. NC inhibitor which were in common with the other miR-378 comparisons were excluded (Fig. 4*B*), and a total of 195 DE genes were identified in the miR-378 inhibitor supplemented group compared to both control groups (Dataset S2). Supplementation of miR-378 inhibitor resulted in 104 DE genes (45 up and 59 down) compared to the nonsupplemented control, and 73 DE genes (36 up and 37 down) compared to the NC inhibitor, while 18 genes were DE for the miR-378 inhibitor group compared to both control groups (*SI Appendix*, Table S6).

Finally, the direct comparison of blastocysts cultured in the presence of the miR-378 mimic vs. miR-378 inhibitor resulted in a total of 145 DE genes (Dataset S3). We compared these DE genes with the above identified DE genes of miR-378 mimic vs. controls ($n = 158$; Dataset S1) and miR-378 inhibitor vs. controls ($n = 195$; Dataset S2) (Fig. 4*C*). A total of 68 DE genes were commonly expressed among these groups, after exclusion of 10 common DE genes between miR-378 mimic and miR-378 inhibitor vs. controls. Hierarchical clustering and heatmap imaging revealed that these 68 significantly altered genes could be categorized into two groups (miR-378 mimic and miR-378 inhibitor) (Fig. 4*D*).

miR-378 Targets Genes Involved in Embryo Quality and Development. To examine the main pathways affected by miR-378, GO gene set overrepresentation analysis was performed with the simplifyEnrichment package (Fig. 5) on the 68 DE genes found both in the direct comparison of miR-378 mimic vs. miR-378 inhibitor and in miR-378 mimic vs. controls and/or in miR-378 inhibitor vs. controls (Fig. 4*C*). This revealed predominant involvement in catabolic and metabolic processes, phosphatase activity, positive regulation, signaling receptor, development, differentiation, and lipoprotein. Additionally, the top 10 KEGG and GO pathways of these common DE genes indicated similar enrichment pathways (as detailed in *SI Appendix*, Fig. S7). In conclusion, both pathway analyses indicated the EV origin of miR-378 and its involvement in embryo development and quality. Additionally, predictive gene target analysis also identified 98 genes (Dataset S4), expressed in human endometrium and regulated by miR-378, which shows that miR-378 could influence embryo implantation.

Discussion

This study proves that EVs secreted by competent embryos contain miR-378a-3p, which significantly affects embryo hatching. We provided evidence for three technical factors: 1) Our customized EV isolation procedure proved effective in isolating EVs from limited volumes of CM, yielding high-quality RNA for robust miRNA sequencing; 2) our data indicated that EV-derived RNAs are more stable than free RNAs derived directly from embryo CM; and 3) we proved that miRNA mimics are able to penetrate embryos without any transfection reagent. This resulted in two major biological findings: 1) The size, morphology, and content of EVs secreted by bovine embryos reflect developmental competence and embryo quality, with blastocyst EVs being larger than nonblastocyst EVs and with differential expression of 21 known and 48 novel miRNAs; 2) miR-378a-3p originates from EVs secreted by

Table 3. Embryo quality assessment of bovine embryos treated with miRNA mimics/inhibitors

Treatment	No. of blastocysts	Cell Nos.				ICM/TCN ratio (%)	AC/TCN ratio (%)
		TCN	ICM	TE	AC		
Control	17	123 ± 9.5[ab]	43.6 ± 3.1[a]	79.8 ± 8.1[a]	8.1 ± 1.3[a]	37.5 ± 2.8[a]	6.4 ± 1.0[a]
NC mimic	16	106 ± 9.8[a]	46.9 ± 3.2[a]	59.1 ± 8.3[a]	5.4 ± 1.4[a]	46.3 ± 2.9[a]	5.0 ± 1.1[a]
miRNA-378 mimic	17	149 ± 9.5[b]	60.1 ± 3.1[b]	88.6 ± 8.1[a]	7.1 ± 1.3[a]	41.3 ± 2.8[a]	4.7 ± 1.0[a]
Control	22	120 ± 7.9[a]	52.3 ± 3.2[a]	68.0 ± 6.1[a]	6.0 ± 1.0[ab]	45.7 ± 2.2[a]	4.9 ± 0.9[ab]
NC inhibitor	17	102 ± 8.9[ab]	42.1 ± 3.7[ab]	60.4 ± 7.0[a]	7.3 ± 1.2[bc]	43.2 ± 2.5[a]	7.2 ± 1.0[bc]
miRNA-378 inhibitor	18	88.3 ± 8.9[b]	38.8 ± 3.6[b]	49.5 ± 6.8[a]	10.2 ± 1.2[c]	44.1 ± 2.5[a]	12.6 ± 1.0[c]

TCN, AC, ICM/TCN ratio, and AC/TCN ratio of differentially stained day 8 blastocysts. For the miRNA mimic experiments, culture media were not supplemented (Control), or were supplemented with control mimics (NC mimics) or miRNA-378 mimics. For the miRNA inhibitor experiment, culture media were not supplemented (Control), or were supplemented with control inhibitors (NC inhibitor) or miRNA-378 inhibitor. Different superscripts per column (a, b, and c) represent statistical differences ($P < 0.05$) among groups. Results are expressed as least-square mean ± SE.

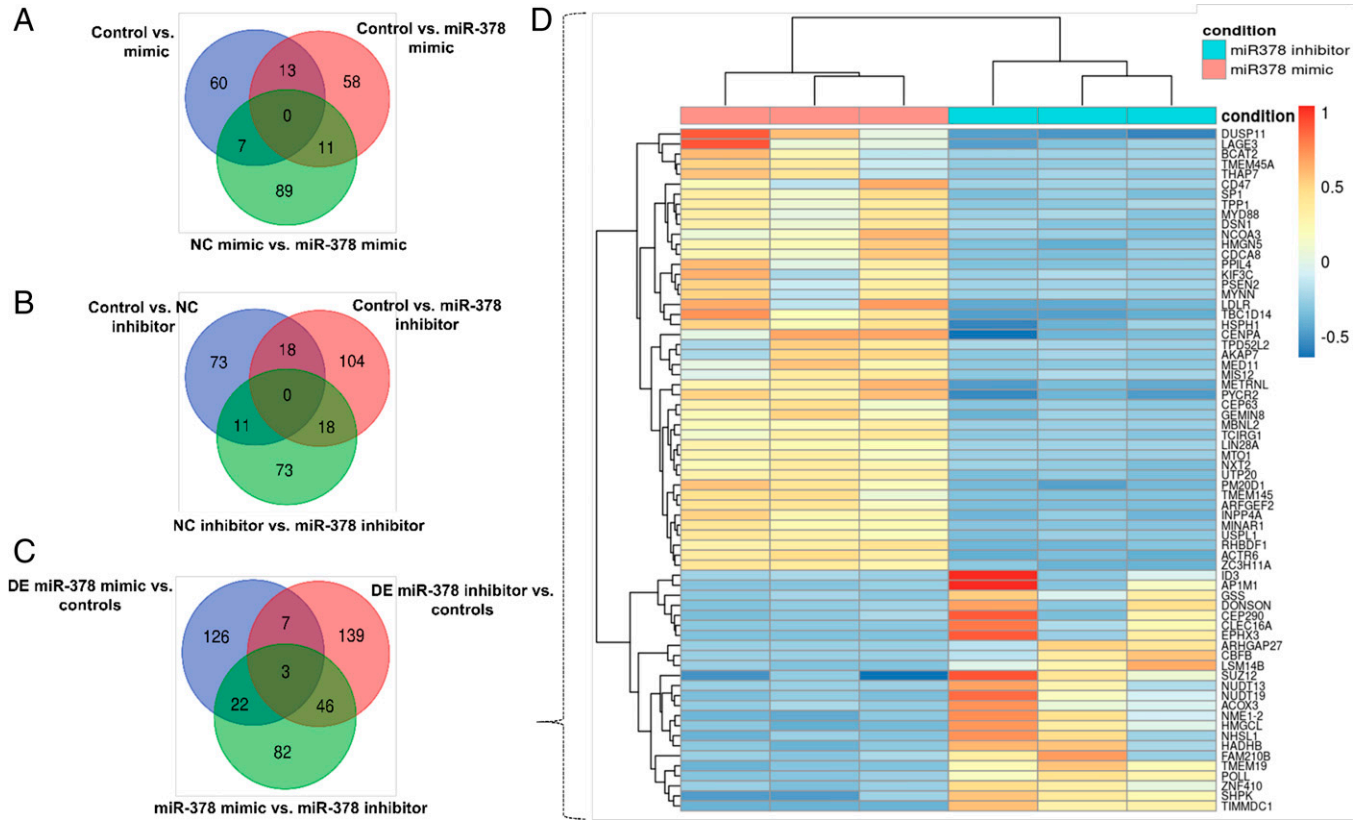

Fig. 4. Venn diagrams showing the number of DE genes in bovine blastocysts after treatment with miR-378 mimic and miR-378 inhibitor vs. NC and unsupplemented controls. (*A*) Control vs. miR-378 mimic vs. NC mimic; (*B*) control vs. miR-378 inhibitor vs. NC inhibitor; (*C*) miR-378 mimic vs. controls, miR-378 inhibitor vs. controls, and miR-378 mimic vs. miR-378 inhibitor. (*D*) Hierarchical clustering (Euclidean distance) and heatmap imaging of the 68 DE genes that are common among DE genes of miR-378 mimic vs. controls or miR-378 inhibitor vs. controls, and miR-378 mimic vs. miR-378 inhibitor. Up-regulated expression is shown in red, and down-regulated expression is shown in blue.

blastocysts and significantly affects embryo quality, hatching, and related gene expression.

There has been a growing interest in embryo-derived EVs and their cargo, but isolating EVs from a limited volume (≤500 μL) of embryo CM is arduous, limiting the yields and purity of EVs obtained by ultracentrifugation protocols (22, 23). In the present study, we used SEC (qEV), which proved to be effective in isolating EVs from limited volumes of bovine embryo CM. In conformity with literature, EV-rich SEC fractions were free from lipoprotein contamination (ApoA-I) (24–26) and from ribonucleoproteins (AGO 2), which might interfere with miRNA sequencing (27, 28). Several recent studies also indicate that SEC (qEV) is a suitable and efficient method for downstream analysis (24, 27, 29–33). However, EVs isolated from low volumes of CM are often not adequate to attain a desirable RNA concentration for miRNA sequencing, and only a few studies have been conducted on miRNAs derived from bovine embryo CM (17, 34, 35). So, in the present study, we optimized a customized procedure for isolating EVs from CM. As it is not possible to use volumes exceeding 1 mL for SEC (qEV), we aliquoted CM into small portions before SEC (qEV). Furthermore, as SEC (qEV) does not result in concentrated samples, we combined it with Ultrafiltration (Amicon), as reported previously (20), to rapidly concentrate the EV fractions instead of pelleting the EVs with an ultracentrifugation step. Overall, this customized procedure proved to be efficient for EV isolation and subsequent RNA extraction (*SI Appendix*, Fig. S3) and miRNA sequencing (*SI Appendix*, Tables S1 and S2).

Our data also indicate that the total RNA content present in EVs is stable and resistant to enzymes that degrade proteins and RNAs, whereas the total RNA content derived directly from CM is relatively less stable and easily degradable by enzymes and detergents, limiting previous studies due to the instability of free circulating miRNAs (36). Therefore, miRNAs originating from EVs are the best choice for starting biomarker studies (37).

Using an individual culture system allowing follow-up of each embryo and collection of corresponding EVs secreted in the medium, we demonstrated that the size, morphology, and content of EVs depend on the embryo development stage and quality. As we selectively collected late fractions with SEC, focusing on isolating small EVs (exosomes and microvesicles), apoptotic bodies were not considered in this study, neither in nonblastocyst nor in blastocyst samples. Hence, among exosomes and microvesicles, blastocyst EVs appear to be larger than nonblastocyst EVs. Smaller-sized EVs in the nonblastocyst group originate from embryos arrested at early stages of embryo development, indicating inferior embryo quality. In conformity, EVs isolated from bovine CM of early embryos (2 dpi and 5 dpi) were relatively small (ranging from 61 nm to 120 nm) compared with EVs collected at 8 dpi (ranging from 154 nm to 163 nm) (22). Interestingly, some of the vesicles are larger than the pores of the zona pellucida in bovine embryos, which are, on average, between 150 nm and 220 nm in diameter, depending on the embryonic stage (38, 39). Our previous study showed fluorescent microspheres of smaller sizes (20 nm to 26 nm) are able to cross the zona of an early blastocyst (40). However, particles with larger sizes (>200 nm) can only pass through the zona when they are

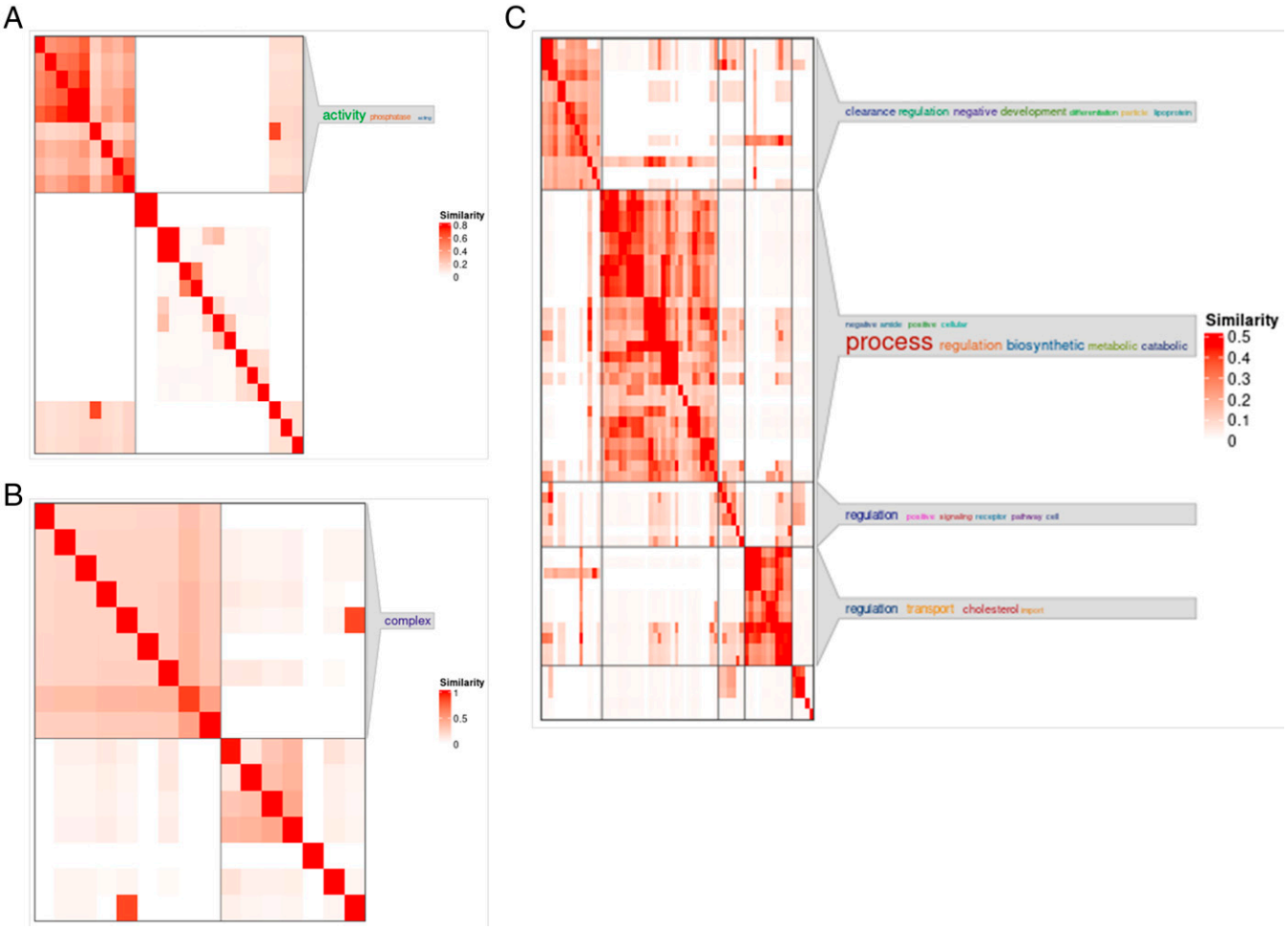

Fig. 5. Overrepresentation analysis on 68 DE genes that were common among miR-378 mimic vs. controls, miR-378 inhibitor vs. controls, and miR-378 mimic vs. miR-378 inhibitor. Semantic similarities scores were calculated between all significant GO terms with their respective category (BP, CC, and MF) with Schlicker's Relevance method. The resulting GO terms were clustered by binary cut enriched (*A*) CC, (*B*) MF, and (*C*) BP.

lipophilic and biologically active (41). This clearly indicates that the EVs are plastic and can adapt and pass through somewhat smaller zona pores.

Besides the morphological difference, we also detected a different miRNA profile in EVs secreted by developmentally competent blastocysts, when compared to EVs derived from medium conditioned by arrested embryos. We identified 21 DE known miRNAs, of which 19 known miRNAs are significantly up-regulated in blastocyst derived EVs. Four of these blastocyst-associated miRNAs have a vital role in embryo development: The miR-378, miR-371, miR-184, and miR-186 form a core set of miRNAs involved in enhancing cell survival and promoting trophoblast cell development (42–44). The miR-378 further regulates trophoblast differentiation and placental development in mice (45), and it has also been detected in human placentas throughout the different stages of gestation and in preterm pregnancies (42). Besides the known miRNAs, 48 novel DE miRNAs were detected. As miRNAs are highly conserved, we could determine 25 mammalian homologs by matching the seed region, but 23 unknown bovine miRNAs require further annotation. Based on miRbase, we identified five blastocyst-associated miRNAs which were connected to the same families (bta-miR-25 and bta-miR-92b to miR-25, and miR-151-3p, bta-miR-151-5p, and bta-miR-28 to miR-28) (*SI Appendix*, Table S1). Both miR-25 and miR-28 are involved in biological processes which are relevant for embryo development, such as cell proliferation, differentiation, migration, and apoptosis (46, 47).

Out of the 21 DE known miRNAs, only two (bta-miR-10b and bta-miR-146b) were up-regulated in nonblastocyst EVs. Our recent bovine studies also identified bta-miR-10b to be up-regulated in medium conditioned by degenerated embryos when compared to medium conditioned by blastocysts (48). The miR-10b negatively influences embryo development and quality by targeting Homeobox A1 (HOXA1) or by influencing DNA methylation (48). However, other studies showed up-regulation of miR-10b in EVs derived from viable bovine embryos (34, 35), which is probably related to a different experimental setup and purification of EVs. In our study, an individual embryo culture system was used, and media were collected based upon the quality of embryos on the final day of embryo culture. In the other studies, media were collected from a group culture system, where embryos were separated at the morula stage and cultured until the blastocyst stage (34, 35). As some morulas might degenerate, there could be an exchange of miRNAs among good and bad embryos during the group culture period, thus compromising the outcome. Overall, an individual culture system allows unbiased sampling and provides the standard for human embryo culture. Besides, in both studies, it is not clear whether miRNA sequencing was performed on EVs or on CM, as the EV purification method was not detailed (34, 35), whereas our customized EV isolation

method proved to be efficient in performing miRNA sequencing from the EVs themselves. In the same way, inconsistencies with other studies showing up-regulation of bta-miR-192, bta-miR-186, and bta-miR-25 in degenerated embryos, while we observed up-regulation in the blastocyst EVs, can be related to the experimental design and to the difference between the analysis of EV-derived miRNAs and free-floating miRNAs (17, 49). Our study also showed an up-regulation of bta-miR-146b in EVs derived from nonblastocysts. The miR-146b has been associated with the promotion of apoptosis and impedes the proliferation of bovine male germline stem cells (50). It directly targets Smad4 pathways and negatively regulates the TGF-β signaling pathway, and, as such, it may eventually affect development of embryonic cells (51).

Further pathway analysis for the 69 DE miRNAs in the general comparison of blastocyst vs. nonblastocyst EVs revealed enrichment of cell development, cell differentiation, cellular proliferation, cell survival, membrane vesicle, and phospholipid binding (Fig. 2 *B–D*). In a previous study, we studied free-floating miRNAs, released directly by bovine embryos into the culture medium, and we mainly detected their involvement in cell death and apoptosis (18). This is in conformity with literature, showing that unbound miRNAs derived directly from embryo CM were generally up-regulated in medium conditioned by degenerated embryos, when compared to blastocyst CM (17, 52). Our data are based upon EV-derived miRNAs and show the opposite, with most of the DE known miRNAs up-regulated in the blastocyst-derived EVs and regulating genes being associated with embryo development, like cell signaling and cellular proliferation. For instance, the MAPK, TGFβ, and Wnt signaling pathways were significantly enriched and participate in protein synthesis, cell survival, migration, invasion, cell cycle progression, cellular proliferation, and differentiation (53–55). Overall, we demonstrate that EVs secreted by blastocysts are larger and contain different miRNAs regulating embryo development when compared to EVs derived from arrested embryos.

To validate these findings, we targeted one of the DE miRNAs for functionality testing. This was preceded by a final technical optimization step. Our data illustrate that fluorescently tagged miRNA mimics can be incorporated by embryonic cells without any transfection reagents. Moreover, these miRNA mimics were stable until the final day of embryo culture (8 dpi), allowing functionality testing by addition of specific miRNA mimics and inhibitors to the embryo culture medium. Incorporation of these miRNAs may be due to the high concentration used in this study following the manufacturer's instruction, but miRNA mimics could also facilitate cellular uptake by endocytosis (56). In our previous study, we observed that specific miRNA mimics (miR-30c and miR-10b) supplemented to the embryo culture medium have a phenotypic influence on embryos, but validation of the embryo uptake mechanism was not performed (18, 48).

The miR-378 proved to significantly enhance embryo quality parameters, and specifically embryo hatching rates, while it also regulated the expression of genes involved in cell division, differentiation and embryo development. The miR-378 was chosen for functionality testing based upon its up-regulation in blastocyst-derived EVs and its key role in enhancing cell survival and promoting trophoblast cell development (42). This was further supported by target gene prediction analysis on miR-378, showing a connection to cell growth, cellular proliferation, and embryo implantation (Table 1). The supplementation of miR-378 mimics significantly improved the embryo hatched/hatching rate, the total number of TE and ICM cells, and the ICM/TCN ratio, whereas addition of the miR-378 inhibitor significantly reduced the embryo hatching rate to almost zero, with concomitant lower embryo quality (Tables 2 and 3).

The association between higher expression of miR-378 and improved embryo quality was further confirmed by qRT-PCR. In conformity with miRNA sequencing data, miR-378 was up-regulated in blastocysts and blastocyst-derived EVs, compared to nonblastocysts and the EVs secreted by these embryos, respectively. Additionally, higher expression of miR-378 in blastocysts cultured in a group compared with individually cultured blastocysts further indicates involvement of miR-378 as an embryotropin in group culture, enhancing hatching. Group culture is able to rescue the development of slow-cleaving embryos (57) and also improves hatching rates (7). While the effect of miR-378 on embryo quality was consistently observed, embryo development rates were not significantly affected, even though the primary selection of miR-378 was based upon its presence in EVs derived from competent embryos that reached the blastocyst stage. It may be that up-regulation of miR-378 is only initiated at the blastocyst stage, implying it affects events occurring after blastulation rather than the chance to reach the blastocyst stage itself. This is supported by the higher miR-378 expression in blastocysts compared to arrested embryos. Additionally, miRNAs enriched in EVs could also be released into CM for the purpose of keeping miRNA homeostasis in embryos to promote survival or with the purpose of communicating with other cells or neighboring embryos in group culture (58).

To further examine the regulating effect of miR-378, miR-378 mimics and inhibitors were supplemented to the embryo culture medium, and the transcriptome of the resulting embryos was analyzed. We identified several common DE genes, resulting from the comparisons of the miR-378 mimic with the controls, the miR-378 inhibitor with the controls, and the miR-378 mimic vs. inhibitor (Fig. 4 and *SI Appendix*, Tables S3 and S4). Based upon pathways analysis, these genes, of which the expression appears affected by miR-378, are involved in cell division, cell differentiation, and embryo development (Fig. 5). Strikingly, among these DE genes, *RAP1GAP* (RAP1 GTPase-activating protein), *NR2C1* (nuclear receptor subfamily 2 group C member 1), *ARFGEF2* (ADP ribosylation factor–guanine nucleotide exchange protein), *SLC7A6* (solute carrier family 7 member 6), *CENPA* (centromere protein A), *SP1* (Sp1 transcription factor), *LDLR* (low-density lipoprotein receptor), *PYCR1* (pyrroline-5-carboxylate reductase 1), *MYD88* (myeloid differentiation factor 88), *TPP1* (tripeptidyl peptidase 1), and *NCOA3* (nuclear receptor coactivator 3) have been shown to play an important role in embryo quality and hatching (59–71). For further evidence and to determine the underlying mechanism of improved hatching, we ran an overrepresentation analysis on these genes. From the enriched pathways (*SI Appendix*, Fig. S8), we could identify the major molecular and enzymatic processes (nuclear receptor, proteases, serine type proteases, nucleosidase, endopeptidase, and reductase) that have been proposed to play a crucial role in the betterment of the hatching process and digestion of the zona pellucida (72–75). As such, transcriptomic profiling of blastocysts treated with miR-378 mimic or inhibitor provided an additional proof that miR-378 regulates the expression of genes involved in embryo quality and hatching. Further, a predictive gene target analysis on miR-378 expressed in human endometrium revealed 98 genes, including *prostaglandin receptor* (*PGR*), which is known to be a crucial gene involved in embryo implantation (76). This indicates that miR-378 might also play a role in embryo implantation by

affecting the endometrium. However, potential off-target effects of the miR-378 mimics and inhibitors cannot be excluded, and further research is required to validate the effect of miR-378 on specific (predicted) target genes, the molecular mechanism behind the effect on hatching, and a potential functional effect of miR-378 on the endometrium.

In summary, the findings presented herein indicate the true potential of EVs derived from preimplantation embryos and their miRNA cargo. This study provides a comprehensive insight into the miRNA content of EVs secreted by blastocysts and nonblastocysts, using an individual culture system. Additionally, we showed that miRNAs originating from EVs are better candidates for embryo quality when compared with free circulating miRNAs or miRNAs of unidentified origin. Notably, EV-derived miR-378 could be a booster for embryo development and quality, since functionality studies proved that it enhances embryo quality and hatching and that it regulates the expression of genes involved in embryo development and quality.

Materials and Methods

Media and Reagents. Tissue culture medium (TCM)-199, minimal essential medium, nonessential amino acids (100×), synthetic basal medium eagle amino acids, gentamycin, and kanamycin were purchased from Life Technologies Europe. PBS was obtained from Gibco (Catalog number: 20012019, Thermo Fisher Scientific). All other chemicals were obtained from Sigma-Aldrich. All media were filtered before use (0.22 μM, Pall Corporation).

In Vitro Embryo Production. An overview of the experimental design is presented in (*SI Appendix*, Fig. S9*A*). Routine in vitro methods were used for bovine embryo production, as described previously by ref. 77 (*SI Appendix*, Fig. S9*A*). Briefly, cow ovaries were obtained at the local abattoir and processed within 2 h after collection. Upon arrival at the laboratory, the ovaries were washed three times in warm physiological saline (with kanamycin [25 mg/mL]). Cumulus–oocyte complexes were aspirated from antral follicles, sizing between 4- and 8-mm diameter, using an 18-gauge needle attached to a 10-mL syringe. Subsequently, viable oocytes with uniformly granulated cytoplasm and surrounded by more than three compact layers of cumulus cells were cultured in groups of 60 in 500 mL of modified bicarbonate buffered TCM-199 (supplemented with 50 mg/mL gentamicin and 20 ng/mL epidermal growth factor) in 5% CO_2 in air for 22 h at 38.5 °C.

Frozen-thawed bull spermatozoa were separated using a 45/90% Percoll gradient (GE Healthcare Biosciences) centrifugation. The sperm pellet was washed in IVF–Tyrode's albumin–pyruvate–lactate (TALP) medium, containing bicarbonate-buffered Tyrode solution. The sperm concentration was adjusted to a final concentration of 1×10^6 spermatozoa per mL using IVF–TALP medium enriched with BSA (Sigma A8806; 6 mg/mL) and heparin (25 mg/mL).

After 22 h of maturation, bovine oocytes were washed in 500 μL of IVF–TALP and subsequently coincubated with bull spermatozoa. After 21-h gamete coincubation, presumed zygotes were vortexed to remove surplus zona attached cumulus and sperm cells. As previously demonstrated by our group, BSA (Sigma A9647) is not a possible source of EV contamination (7). So, 4 mg/mL BSA (Sigma A9647) was supplemented to synthetic oviductal fluid enriched with nonessential and essential amino acids (SOFaa) and ITS (5 μg/mL insulin; 5 μg/mL transferrin; 5 ng/mL selenium). The presumed zygotes were culture individually in 20-μL droplets, or in groups of 25 in 50-μL droplets (control) covered with Paraffin oil (SAGE oil for tissue culture, ART-4008-5P, Cooper Surgical Company), at 38 °C in 5% CO_2, 5% O_2, and 90% N_2.

In total, individual droplets of 2,520 presumed zygotes (nine replicates) were cultured. Three replicates with 120 presumed zygotes were performed for EV characterization, and six replicates with 360 presumed zygotes for miRNA analysis. At 45 h post insemination, embryo cleavage was scored as the percentage of cleaved embryos out of presumed zygotes. At 8 dpi, the developmental competence of each embryo was assessed, enabling a division of individually cultured embryos into two subgroups: 1) embryos that were not able to reach the blastocyst stage (nonblastocysts) and 2) blastocysts. CM of individually cultured blastocysts or nonblastocysts were pooled into two groups, each containing a total of nine replicates, used for further analysis (*SI Appendix*, Fig. S9).

Media Collection from Individually Cultured Embryos. For EV isolation and characterization, three replicates of 500 μL of CM were collected from each group (blastocyst or nonblastocyst). To obtain 500 μL of CM, 26 individual culture droplets of CM were pooled according to embryo development (as illustrated in *SI Appendix*, Fig. S9). A maximum volume of 500 μL (one replicate) from each group was subjected to SEC (qEV single column). Similarly, for total RNA and miRNA extraction from EVs, six replicates with 2 mL of pooled CM from each group (blastocyst or nonblastocyst) were collected. To obtain 2 mL of CM, 110 individual culture droplets of CM were pooled for both blastocysts and nonblastocysts. As illustrated in (*SI Appendix*, Fig. S9*B*), EV isolation was performed by splitting 2 mL (one replicate) of blastocyst or nonblastocyst CM into four groups of 500 μL each. Eluted EV-rich fractions (6 to 15) of each group were subjected to an Amicon Ultra-2 10K filter (UFC201024, Merck Millipore) for concentration. Finally, 600 μL of the EV concentrated pellet was subjected to total RNA extraction followed by miRNA extraction. The same procedure was performed for the other five replicates for miRNA isolation.

EV Isolation by qEV Single Column. EVs were isolated by qEV single size exclusion column (IZON Science, Cat. Number: qEV single ser. Y1000588). A maximum 500 μL of blastocyst or nonblastocyst CM was loaded onto the qEV Classic size exclusion column, followed by elution with 5 mL of freshly filtered PBS (PH: 7.4, 0.22 μm filtered). As per the manufacturer's instructions, EV-rich fractions 6 to 15 were pooled and loaded in Amicon Ultra-2 10 K centrifugal filters (UFC201024, Merck Millipore) and centrifuged at 4 °C for 40 min at 3,000 × *g* using a swinging bucket rotor. Concentration of the samples was achieved by upside-down centrifugation at 4 °C for 2 min at 1,000 × *g* (7). Around 200 μL of EVs were retrieved from the flow-through reservoir and stored at −80 °C until downstream analysis. These EVs will hereinafter be called blastocyst EVs and nonblastocyst EVs, referring to their origin.

Extracellular Vesicles Characterization. All the EVs identification and characterization methods (western blotting, transmission electron microscopy, nanoparticle tracking analysis) are detailed in *SI Appendix*.

RNA Isolation and RNA Analyses. Purified EVs were extracted from the CM from both groups (blastocyst and nonblastocyst) by qEV single size exclusion column. As detailed above (illustrated in *SI Appendix*, Fig. S9*B*), 600 μL (× 6 replicates) of the concentrated EV pellet from each group was used for total RNA extraction, using the Plasma/Serum Circulating & Exosomal RNA Purification Mini Kit (Norgen Biotek, Cat. 51000) according to the manufacturer's protocol. The quality and concentration of the RNA samples were examined using an RNA 6000 Pico Chip (Agilent Technologies) and a Quant-iT RiboGreen RNA Assay kit (Life Technologies), respectively.

Small RNA Library Construction and Deep Sequencing. Small RNA library preparation was performed with the Tailormix v2 kit (SeqMatic). The quality-ensured RNA-seq libraries were pooled, and sequencing was performed in triplicate (of x 6 replicates) (*SI Appendix*, Fig. S9*B*) on the Illumina Miseq (NXTGNT sequencing facility of Ghent University). Quality control included sequence quality, sequencing depth, read duplication rates (clonal reads), alignment quality, and nucleotide composition bias.

Small RNA-seq Data Analysis. Identification of known miRNAs, prediction of putative novel miRNAs, and read counting were done using the mirPRo pipeline (78). The microRNA data from the miRBase (v22) (79) and the annotated cow genome (Bos Taurus ARS-UCD1.2 release 95) were used as a reference. Prior to the small RNA-seq, one replicate of the nonblastocyst EVs sample did not meet the quality control metrics (*SI Appendix*, Fig. S3*D*), so we removed this samples from the analysis. Differential expression between blastocyst EVs (three replicates) and nonblastocyst EVs (two replicates) was statistically tested in R (R version 4.0.3) (80) with DESeq2 (81) via a custom written R script. A miRNA was considered DE when the Benjamini–Hochberg corrected *P* value was ≤ 0.05 and the absolute value of the $\log_2$ foldchange was ≥ 1. The heatmap of DE miRNAs was constructed by

selecting the DE miRNAs. Expression values were normalized with the median ratio method and subsequently transformed with a variance stabilizing transformation, both as implemented in DESeq2. The mean transformed expression value over all samples was subtracted from the transformed expression value of each sample.

Target Gene Prediction and GO/KEGG Pathway Enrichment Analysis. Based on the sequence of the DE miRNAs (from nonblastocyst EVs and blastocyst EVs) and the 3′ untranslated regions of the bovine transcripts potential target mRNAs were determined using miRanda v3.3a (82). These initial results were filtered based on their paired score (>155) and energy (<−20). To gain further biological insight into these results, a classical overrepresentation analysis based on a hypergeometric test was applied in the R package fgsea (83). Pathways with a P value ≤ 0.05 were considered statistically significant. GO terms contain redundant information due to their hierarchical nature. To avoid this redundancy, the initial results of the enrichment analysis were processed further by calculating semantic similarities between the significant GO terms with the relevance method (84). Afterward, clustering was performed with the binary cut method. Both steps were implemented in the R package simplifyEnrichment (85). Additional details of sequence annotation pipeline analysis and predictive gene target analysis on miR-378 connecting to endometrium are described in *SI Appendix*.

Confirmation of EV Origin. Details on EVs degradation and determining miR-378 origin are described in *SI Appendix*.

miRNA Functional Analysis. Details of miRNA functional analysis are provided in *SI Appendix*.

Labeling and Uptake. Bovine embryos were produced in vitro as specified above in *In Vitro Embryo Production*, and embryo culture was performed in groups of 25 embryos in 50-μL droplets of SOF+ITS+BSA, covered with mineral oil at 38.5 °C in 5% CO_2, 5% O_2, and 90% N_2. Fluorescently labeled NC miRNA mimics (miRCURY LNA miRNA Mimic - 5′ Fam, Product No. 339173, Qiagen) were supplemented into the culture medium of presumed zygotes (*SI Appendix*, Fig. S9*C*, *Top*) with a final concentration of 1 μM (as per the miRCURY LNA miRNA Mimics Handbook). In parallel, a control was included by adding an equal volume of RNA-free water to culture medium. On 2 and 8 dpi, the embryos were washed twice using PBS–BSA and fixed at room temperature for 30 min with 4% paraformaldehyde. All embryos were stained with Hoechst 33342 (dilution 1:100 PBS) for 10 min and imaged using a ZEISS Confocal Microscope (ZEISS LSM 980, Zeiss Microscopy). This experiment was repeated three times, and 15 to 20 embryos were assessed per replicate.

Supplementing miR-378 Mimics and Inhibitors. The microRNA mimics and inhibitors with a unique LNA-enhanced, triple-RNA strand designed for mimicking mature endogenous miR-378 (has-miR-378a-3p) were purchased from Qiagen. These miR-378 mimics and inhibitors (miRCURY LNA Power mimics and inhibitors, Product Nos. 339173 and 339131, respectively) were supplemented to the culture medium of presumed zygotes (n = 1,155, eight replicates) (*SI Appendix*, Fig. S9*C*, *Bottom*) with a final concentration of 1 μM. In parallel, an NC mimic or inhibitor (cel-miR-39-3p, labeled miRNA mimic and inhibitor, Product No. 339173, Qiagen) was supplemented to the culture medium. Finally, a control group was included by adding an equal volume of RNA-free water to culture medium.

In vitro embryo culture was performed in two treatments (mimic and inhibitor). For the mimic treatment, the presumed zygotes (n = 557, four replicates) were allocated to three different groups (control, NC mimic, and miR-378 mimic). Similarly, for the inhibitor treatment, the presumed zygotes (n = 598, four replicates) were allocated to three different groups (control, NC inhibitor, and miR-378 inhibitor). Culture medium was prepared in groups, as described above, by culturing 25 embryos in 50-μL droplets of SOF+ITS+BSA, covered with mineral oil at 38.5 °C in 5% CO_2, 5% O_2, and 90% N_2. Embryo development was evaluated on 7 and 8 dpi, while embryo quality was assessed by differential staining on 8 dpi. All blastocysts (8 dpi) were collected for differential apoptotic staining and transcriptomic analysis.

Differential Apoptotic Staining. Differential apoptotic staining was performed using a previously described protocol (86). A brief description is provided in *SI Appendix*.

qRT-PCR Analysis. Total RNA (including small RNA) was isolated from blastocysts and nonblastocyst embryos derived from both group and individual culture (three replicates of eight embryos in each group), using the miRNeasy mini kit (Qiagen). Reverse transcription, qRT-PCR, and data analysis were performed as reported previously (18). A brief description is provided in *SI Appendix*.

Transcriptomics. Details on transcriptomics analysis are provided in *SI Appendix*.

Availability of Protocols. Written details on experimental procedures have been submitted to the Transparent reporting and Centralizing Knowledge in Extracellular Vesicle Research (EV-TRACK) knowledgebase (EVTRACK ID: EV200029) .

Statistical Analyses. Details of statistical analyses are provided in *SI Appendix*.

Data Availability. The miRNA sequencing and transcriptomics datasets generated during the current study were deposited in the National Center for Biotechnology Information (NCBI) Gene Expression Omnibus (GEO) database with accession number GSE197878. Written details on experimental procedures have been submitted to the EV-TRACK knowledgebase (EVTRACK ID: EV200029) (87). All other study data are included in the article and/or supporting information.

ACKNOWLEDGMENTS. We thank Petra Van Damme and Sofie De Geyter for their excellent technical assistance. We thank Rocío Melissa Rivera from the University of Missouri for her careful revision of the manuscript. This work was supported by Ghent University (Grant: Bijzonder Onderozoeksfonds Geconcerteerde Onderzoeksactie 2018000504 [GOA030-18 BOF]) and by the European Union (H2020 Marie Sklodowska-Curie Innovative Training Network: project Biology and Technology of Reproductive Health or REP-BIOTECH 675526). K.C.P. is supported by Fonds Wetenschappelijk Onderzoek: Grant 1228821N; O.B.P. is supported by Fonds Wetenschappelijk Onderzoek: Grant 12Y5220N. The confocal microscope was supported by grants to B.H. (FWO.HMZ.2016.0002.01, Hercules project and UGent BOF.BAS.2018.0018.01).

Author affiliations: [a]Department of Reproduction, Obstetrics and Herd Health, Faculty of Veterinary Medicine, University of Ghent, B-9820 Merelbeke, Belgium; [b]Department for Reproductive Medicine, Ghent University Hospital, 9000 Gent, Belgium; [c]Department of Pharmaceutics, Faculty of Pharmaceutical Sciences, Ghent University, B-9000 Ghent, Belgium; [d]Department of Veterinary Sciences, Gamete Research Center, University of Antwerp, 2610 Antwerp, Belgium; [e]Department of Nutrition, Genetics and Ethology, Faculty of Veterinary Medicine, Ghent University, B-9000 Ghent, Belgium; [f]Institute of Crop Science and Resource Conservation, Plant Pathology, Rheinische Friedrich-Wilhelms-University of Bonn, D-53115 Bonn, Germany; [g]Ghent-Fertility and Stem Cell Team, Department for Reproductive Medicine, Ghent University Hospital, 9000 Ghent, Belgium; [h]Department of Biomolecular Health Sciences, Faculty of Veterinary Medicine, Utrecht University, 3584 CM Utrecht, The Netherlands; [i]Laboratory of Experimental Cancer Research, Department of Human Structure and Repair, Ghent University, B-9000 Ghent, Belgium; and [j]Cancer Research Institute Ghent, B-9000 Ghent, Belgium

1. M. Okabe, Sperm-egg interaction and fertilization: Past, present, and future. *Biol. Reprod.* **99**, 134–146 (2018).
2. J. Marcos *et al.*, Collapse of blastocysts is strongly related to lower implantation success: A time-lapse study. *Hum. Reprod.* **30**, 2501–2508 (2015).
3. M. E. Hammadeh, C. Fischer-Hammadeh, K. R. Ali, Assisted hatching in assisted reproduction: A state of the art. *J. Assist. Reprod. Genet.* **28**, 119–128 (2011).
4. P. Ramos-Ibeas *et al.*, Senescence and apoptosis during *in vitro* embryo development in a bovine model. *Front. Cell Dev. Biol.* **8**, 619902 (2020).
5. E. R. Norwitz, D. J. Schust, S. J. Fisher, Implantation and the survival of early pregnancy. *N. Engl. J. Med.* **345**, 1400–1408 (2001).
6. D. Li *et al.*, Effect of assisted hatching on pregnancy outcomes: A systematic review and meta-analysis of randomized controlled trials. *Sci. Rep.* **6**, 31228 (2016).
7. K. C. Pavani *et al.*, Isolation and characterization of functionally active extracellular vesicles from culture medium conditioned by bovine embryos in vitro. *Int. J. Mol. Sci.* **20**, E38 (2018).
8. J. C. da Silveira, D. N. R. Veeramachaneni, Q. A. Winger, E. M. Carnevale, G. J. Bouma, Cell-secreted vesicles in equine ovarian follicular fluid contain miRNAs and proteins: A possible new form of cell communication within the ovarian follicle1. *Biol. Reprod.* **86**, 71 (2012).
9. M. Simons, G. Raposo, Exosomes–Vesicular carriers for intercellular communication. *Curr. Opin. Cell Biol.* **21**, 575–581 (2009).
10. K. C. Pavani *et al.*, Emerging role of extracellular vesicles in communication of preimplantation embryos *in vitro*. *Reprod. Fertil. Dev.* **29**, 66–83 (2016).
11. I. M. Saadeldin, S. J. Kim, Y. B. Choi, B. C. Lee, Improvement of cloned embryos development by co-culturing with parthenotes: A possible role of exosomes/microvesicles for embryos paracrine communication. *Cell. Reprogram.* **16**, 223–234 (2014).

12. R. Lopera-Vásquez *et al.*, Extracellular vesicles from BOEC in in vitro embryo development and quality. *PLoS One* **11**, e0148083 (2016).
13. K. Dissanayake *et al.*, Oviduct as a sensor of embryo quality: Deciphering the extracellular vesicle (EV)-mediated embryo-maternal dialogue. *J. Mol. Med. (Berl.)* **99**, 685–697 (2021).
14. K. Godakumara *et al.*, Trophoblast derived extracellular vesicles specifically alter the transcriptome of endometrial cells and may constitute a critical component of embryo-maternal communication. *Reprod. Biol. Endocrinol.* **19**, 115 (2021).
15. C. Théry, Cancer: Diagnosis by extracellular vesicles. *Nature* **523**, 161–162 (2015).
16. V. Vlaeminck-Guillem, Extracellular vesicles in prostate cancer carcinogenesis, diagnosis, and management. *Front. Oncol.* **8**, 222 (2018).
17. J. Kropp, S. M. Salih, H. Khatib, Expression of microRNAs in bovine and human pre-implantation embryo culture media. *Front. Genet.* **5**, 91 (2014).
18. X. Lin *et al.*, Bovine embryo-secreted microRNA-30c is a potential non-invasive biomarker for hampered preimplantation developmental competence. *Front. Genet.* **10**, 315 (2019).
19. J. Kowal *et al.*, Proteomic comparison defines novel markers to characterize heterogeneous populations of extracellular vesicle subtypes. *Proc. Natl. Acad. Sci. U.S.A.* **113**, E968–E977 (2016).
20. A. Asaadi *et al.*, Extracellular vesicles from follicular and ampullary fluid isolated by density gradient ultracentrifugation improve bovine embryo development and quality. *Int. J. Mol. Sci.* **22**, E578 (2021).
21. I.-S. Bae *et al.*, Identification of reference genes for relative quantification of circulating microRNAs in bovine serum. *PLoS One* **10**, e0122554 (2015).
22. K. Dissanayake *et al.*, Individually cultured bovine embryos produce extracellular vesicles that have the potential to be used as non-invasive embryo quality markers. *Theriogenology* **149**, 104–116 (2020).
23. K. C. Pavani *et al.*, The separation and characterization of extracellular vesicles from medium conditioned by bovine embryos. *Int. J. Mol. Sci.* **21**, E2942 (2020).
24. A. N. Böing *et al.*, Single-step isolation of extracellular vesicles by size-exclusion chromatography. *J. Extracell. Vesicles* **3**, 10.3402/jev.v3.23430 (2014).
25. R. J. Lobb *et al.*, Optimized exosome isolation protocol for cell culture supernatant and human plasma. *J. Extracell. Vesicles* **4**, 27031 (2015).
26. K. Takov, D. M. Yellon, S. M. Davidson, Comparison of small extracellular vesicles isolated from plasma by ultracentrifugation or size-exclusion chromatography: Yield, purity and functional potential. *J. Extracell. Vesicles* **8**, 1560809 (2018).
27. Y. Yang *et al.*, Extracellular vesicles isolated by size-exclusion chromatography present suitability for RNomics analysis in plasma. *J. Transl. Med.* **19**, 104 (2021).
28. J. Van Deun *et al.*, The impact of disparate isolation methods for extracellular vesicles on downstream RNA profiling. *J. Extracell. Vesicles* **3**, 10.3402/jev.v3.24858 (2014).
29. L. Antounians *et al.*, The regenerative potential of amniotic fluid stem cell extracellular vesicles: Lessons learned by comparing different isolation techniques. *Sci. Rep.* **9**, 1837 (2019).
30. G. K. Patel *et al.*, Comparative analysis of exosome isolation methods using culture supernatant for optimum yield, purity and downstream applications. *Sci. Rep.* **9**, 5335 (2019).
31. R. Stranska *et al.*, Comparison of membrane affinity-based method with size-exclusion chromatography for isolation of exosome-like vesicles from human plasma. *J. Transl. Med.* **16**, 1 (2018).
32. S. Ebrahimkhani *et al.*, Deep sequencing of circulating exosomal microRNA allows non-invasive glioblastoma diagnosis. *NPJ Precis. Oncol.* **2**, 28 (2018).
33. S. Ebrahimkhani *et al.*, Exosomal microRNA signatures in multiple sclerosis reflect disease status. *Sci. Rep.* **7**, 14293 (2017).
34. E. A. Mellisho *et al.*, Extracellular vesicles secreted during blastulation show viability of bovine embryos. *Reproduction* **158**, 477–492 (2019).
35. B. Melo-Baez *et al.*, MicroRNAs from extracellular vesicles secreted by bovine embryos as early biomarkers of developmental competence. *Int. J. Mol. Sci.* **21**, E8888 (2020).
36. X. Lin, "Bovine in vitro embryo secreted-miRNAs as potential non-invasive biomarkers for preimplantation developmental competence," PhD thesis, Ghent University, Merelbeke, Belgium (2019).
37. N. N. S. B. Nik Mohamed Kamal, W. N. S. Shahidan, Non-exosomal and exosomal circulatory microRNAs: Which are more valid as biomarkers? *Front. Pharmacol.* **10**, 1500 (2020).
38. G. Vanroose, A. de Kruif, A. Van Soom, Embryonic mortality and embryo-pathogen interactions. *Anim. Reprod. Sci.* **60–61**, 131–143 (2000).
39. A. Van Soom *et al.*, Sucrose-induced shrinkage of in vitro produced bovine morulae: Effect on viability, morphology and ease of evaluation. *Theriogenology* **46**, 1131–1147 (1996).
40. B. Mateusen *et al.*, Susceptibility of pig embryos to porcine circovirus type 2 infection. *Theriogenology* **61**, 91–101 (2004).
41. K. Turner, R. W. Horobin, Permeability of the mouse zona pellucida: A structure-staining-correlation model using coloured probes. *J. Reprod. Fertil.* **111**, 259–265 (1997).
42. L. Luo *et al.*, MicroRNA-378a-5p promotes trophoblast cell survival, migration and invasion by targeting Nodal. *J. Cell Sci.* **125**, 3124–3132 (2012).
43. S. Suman *et al.*, Alteration of miR-186 expression modifies inflammatory markers in normal epithelial and prostate cancer cell models. *FASEB J.* **31**, 757.716 (2017).
44. H. Wang *et al.*, MiR-371 promotes proliferation and metastasis in hepatocellular carcinoma by targeting PTEN. *BMB Rep.* **52**, 312–317 (2019).
45. H. Hayder, J. O'Brien, U. Nadeem, C. Peng, MicroRNAs: Crucial regulators of placental development. *Reproduction* **155**, R259–R271 (2018).
46. M. Sárközy, Z. Kahán, T. Csont, A myriad of roles of miR-25 in health and disease. *Oncotarget* **9**, 21580–21612 (2018).
47. C. Schneider *et al.*, MicroRNA 28 controls cell proliferation and is down-regulated in B-cell lymphomas. *Proc. Natl. Acad. Sci. U.S.A.* **111**, 8185–8190 (2014).
48. X. Lin *et al.*, Bta-miR-10b secreted by bovine embryos negatively impacts preimplantation embryo quality. *Front. Genet.* **10**, 757 (2019).
49. J. Kropp, H. Khatib, mRNA fragments in in vitro culture media are associated with bovine preimplantation embryonic development. *Front. Genet.* **6**, 273 (2015).
50. N. Li *et al.*, Expression of miRNA-146b-5p in patients with thyroid cancer in combination with Hashimoto's disease and its clinical significance. *Oncol. Lett.* **17**, 4871–4876 (2019).
51. N. Zhang *et al.*, miR-146b-5p promotes the neural conversion of pluripotent stem cells by targeting Smad4. *Int. J. Mol. Med.* **40**, 814–824 (2017).
52. J. Kropp, H. Khatib, Characterization of microRNA in bovine in vitro culture media associated with embryo quality and development. *J. Dairy Sci.* **98**, 6552–6563 (2015).
53. S.-Y. Kim, K.-H. Baek, TGF-β signaling pathway mediated by deubiquitinating enzymes. *Cell. Mol. Life Sci.* **76**, 653–665 (2019).
54. A. V. Timofeeva *et al.*, Cell-free, embryo-specific sncRNA as a molecular biological bridge between patient fertility and IVF efficiency. *Int. J. Mol. Sci.* **20**, E2912 (2019).
55. X. Varelas *et al.*, TAZ controls Smad nucleocytoplasmic shuttling and regulates human embryonic stem-cell self-renewal. *Nat. Cell Biol.* **10**, 837–848 (2008).
56. J. F. Wiggins *et al.*, Development of a lung cancer therapeutic based on the tumor suppressor microRNA-34. *Cancer Res.* **70**, 5923–5930 (2010).
57. E. Wydooghe *et al.*, Replacing serum in culture medium with albumin and insulin, transferrin and selenium is the key to successful bovine embryo development in individual culture. *Reprod. Fertil. Dev.* **26**, 717–724 (2014).
58. H. Geekiyanage, S. Rayatpisheh, J. A. Wohlschlegel, R. Brown Jr., V. Ambros, Extracellular microRNAs in human circulation are associated with miRISC complexes that are accessible to anti-AGO2 antibody and can bind target mimic oligonucleotides. *Proc. Natl. Acad. Sci. U.S.A.* **117**, 24213–24223 (2020).
59. B. M. Bany, C. A. Scott, K. S. Eckstrum, Analysis of uterine gene expression in interleukin-15 knockout mice reveals uterine natural killer cells do not play a major role in decidualization and associated angiogenesis. *Reproduction* **143**, 359–375 (2012).
60. G. Kakourou *et al.*, Investigation of gene expression profiles before and after embryonic genome activation and assessment of functional pathways at the human metaphase II oocyte and blastocyst stage. *Fertil. Steril.* **99**, 803–814.e23 (2013).
61. P. Grzmil *et al.*, Early embryonic lethality in gene trap mice with disruption of the Arfgef2 gene. *Int. J. Dev. Biol.* **54**, 1259–1266 (2010).
62. N. Forde *et al.*, Amino acids in the uterine luminal fluid reflects the temporal changes in transporter expression in the endometrium and conceptus during early pregnancy in cattle. *PLoS One* **9**, e100010 (2014).
63. F. W. Bazer *et al.*, The many faces of interferon tau. *Amino Acids* **47**, 449–460 (2015).
64. A. Gely-Pernot *et al.*, Gestational exposure to chlordecone promotes transgenerational changes in the murine reproductive system of males. *Sci. Rep.* **8**, 10274 (2018).
65. G. Ambartsumyan *et al.*, Centromere protein A dynamics in human pluripotent stem cell self-renewal, differentiation and DNA damage. *Hum. Mol. Genet.* **19**, 3970–3982 (2010).
66. X. Zhang *et al.*, Sp1-regulated transcription of RasGRP1 promotes hepatocellular carcinoma (HCC) proliferation. *Liver Int.* **38**, 2006–2017 (2018).
67. J. Herz, D. E. Clouthier, R. E. Hammer, LDL receptor-related protein internalizes and degrades uPA-PAI-1 complexes and is essential for embryo implantation. *Cell* **71**, 411–421 (1992).
68. M.-L. Kuo *et al.*, PYCR1 and PYCR2 interact and collaborate with RRM2B to protect cells from overt oxidative stress. *Sci. Rep.* **6**, 18846 (2016).
69. W. Lei, H. Ni, J. Herington, J. Reese, B. C. Paria, Alkaline phosphatase protects lipopolysaccharide-induced early pregnancy defects in mice. *PLoS One* **10**, e0123243 (2015).
70. L. L. Santos, C. K. Ling, E. Dimitriadis, Tripeptidyl peptidase I promotes human endometrial epithelial cell adhesive capacity implying a role in receptivity. *Reprod. Biol. Endocrinol.* **18**, 124 (2020).
71. Z. Wu *et al.*, Role of nuclear receptor coactivator 3 (Ncoa3) in pluripotency maintenance. *J. Biol. Chem.* **287**, 38295–38304 (2012).
72. H. J. Kang *et al.*, Activation of peroxisome proliferators-activated receptor δ (PPARδ) promotes blastocyst hatching in mice. *Mol. Hum. Reprod.* **17**, 653–660 (2011).
73. G. Sireesha *et al.*, Role of cathepsins in blastocyst hatching in the golden hamster. *Mol. Hum. Reprod.* **14**, 337–346 (2008).
74. E. D. Aflalo, U. A. Sod-Moriah, G. Potashnik, I. Har-Vardi, Expression of plasminogen activators in preimplantation rat embryos developed in vivo and in vitro. *Reprod. Biol. Endocrinol.* **3**, 7 (2005).
75. N. Sharma *et al.*, Implantation Serine Proteinases heterodimerize and are critical in hatching and implantation. *BMC Dev. Biol.* **6**, 61 (2006).
76. S.-P. Wu, R. Li, F. J. DeMayo, Progesterone receptor regulation of uterine adaptation for pregnancy. *Trends Endocrinol. Metab.* **29**, 481–491 (2018).
77. E. Wydooghe *et al.*, Individual commitment to a group effect: Strengths and weaknesses of bovine embryo group culture. *Reproduction* **148**, 519–529 (2014).
78. J. Shi *et al.*, mirPRo–A novel standalone program for differential expression and variation analysis of miRNAs. *Sci. Rep.* **5**, 14617–14617 (2015).
79. S. Griffiths-Jones, R. J. Grocock, S. van Dongen, A. Bateman, A. J. Enright, miRBase: MicroRNA sequences, targets and gene nomenclature. *Nucleic Acids Res.* **34**, D140–D144 (2006).
80. R. Ihaka, R. Gentleman, R: A language for data analysis and graphics. *J. Comput. Graph. Stat.* **5**, 299–314 (1996).
81. M. I. Love, W. Huber, S. Anders, Moderated estimation of fold change and dispersion for RNA-seq data with DESeq2. *Genome Biol.* **15**, 550 (2014).
82. D. Betel, A. Koppal, P. Agius, C. Sander, C. Leslie, Comprehensive modeling of microRNA targets predicts functional non-conserved and non-canonical sites. *Genome Biol.* **11**, R90 (2010).
83. G. Korotkevich, V. Sukhov, A. Sergushichev, Fast gene set enrichment analysis, version 3. bioRxiv [Preprint] (2019). https://doi.org/10.1101/060012. Accessed 10 March 2022.
84. A. Schlicker, F. S. Domingues, J. Rahnenführer, T. Lengauer, A new measure for functional similarity of gene products based on Gene Ontology. *BMC Bioinformatics* **7**, 302 (2006).
85. Z. Gu, D. Hübschmann, simplifyEnrichment: An R/Bioconductor package for Clustering and Visualizing Functional Enrichment Results, version 2. bioRxiv [Preprint] (2021). https://doi.org/10.1101/2020.10.27.312116. Accessed 10 March 2022.
86. E. Wydooghe *et al.*, Differential apoptotic staining of mammalian blastocysts based on double immunofluorescent CDX2 and active caspase-3 staining. *Anal. Biochem.* **416**, 228–230 (2011).
87. J. Van Deun *et al.*; EV-TRACK Consortium, EV-TRACK: Transparent reporting and centralizing knowledge in extracellular vesicle research. *Nat. Methods* **14**, 228–232 (2017).